THE JOURNAL OF PHYSICAL CHEMISTRY B

Article

Cite This: J. Phys. Chem. B 2017, 121, 10344-10352

pubs.acs.org/JPCB

Mechanisms of Activation and Subunit Release in Ca^{2+}/Calmodulin-Dependent Protein Kinase II

Filippo Pullara,[†,¶] Eliana K. Asciutto,[‡,¶] and Ignacio J. General*[,‡]

[†]Department of Computational and Systems Biology, School of Medicine, University of Pittsburgh, Pittsburgh, Pennsylvania 15260, United States

[‡]School of Science and Technology, Universidad Nacional de San Martin, and CONICET, 25 de Mayo y Francia, San Martín, 1650 Buenos Aires, Argentina

ABSTRACT: Calcium/calmodulin-dependent protein kinase II is an enzyme involved in many different functions, including the so-called long-term potentiation, a mechanism that strengthens synapses in a persistent mode and is believed to be a basic cellular mechanism for memory formation. Here we study the conformational changes of the enzyme due to phosphorylation of some key residues that are believed to drive the transition from an inhibited to an active state; it is this active state the one associated with long-term potentiation. We found that the conformational changes could be explained in terms of three charged regions in the three main subdomains of the enzyme: the hub, linker, and kinase. The role of phosphorylation is to change the charge relation between them, turning on and off their interactions and switching between an attractive state (nonphosphorylated or inhibited) and a not attractive one (phosphorylated or active). We also show that phosphorylated subunits become less stable, and this could favor their release from the multimer, as has been already observed experimentally.

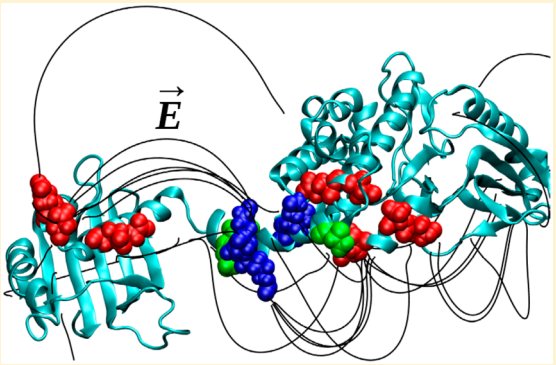

INTRODUCTION

Calcium/calmodulin (Ca/CaM)-dependent protein kinase II, CaMKII, is a serine/threonine-specific kinase, which is regulated by the Ca/CaM complex. This enzyme is involved in many biological processes, such as calcium regulation,[1] signal transduction in epithelia,[2] the cell cycle,[3] and T-cell activation.[4] However, one of the most important aspects of CaMKII, for which it is and has been actively studied, is related to the regulation of certain neuronal processes, including long-term potentiation (LTP), i.e., the enhancement of synapses related to memory formation.[5]

There are 4 CaMKII genes in humans, α, β, γ, and δ, which are expressed in at least 38 isoforms,[6] through alternative splicing. There is a large sequence identity between the different human isoforms, and the largest difference is found in the length of the linker connecting the C and N domains: it can have a large variation in size, and this change affects the frequency response of CaMKII to Ca/CaM pulses.[7] In this work, we study the α isoform of CaMKII, predominantly found in the brain, with a β7 linker, which has been shown to have a reduced kinase activity.[8]

Structurally, the variant of CaMKII that we study in this work is a dodecamer, composed of two rings, stacked one on top of the other, and each formed by six subunits (SUs). Each SU of the system is composed of three subdomains: the C-terminal hub (H), located toward the center of the ring, forming the core of the system; the linker (L) connecting H with the exterior part of the SU; and the N-terminal kinase (K). These Ks are responsible for the phosphorylation of other neighboring kinases, both in the same dodecamer and in others. Their activity depends on the overall structure of the SU. That is, a closed conformation, where K is docked onto H, does not allow the flexibility that a kinase needs in order to phosphorylate its neighbors, and thus, it is called an autoinhibited structure. On the other hand, an open conformation, with K moving away from H, allows for an active kinase.

Hence, the activation process is thought to begin with a SU in a closed form, with its K domain docked onto H. Ca/CaM binds around amino acids T305/306, resulting in the displacement of an inhibitory regulatory segment and opening of the SU (see Figure 1, right panel). This is followed by phosphorylation of T286, which inhibits rebinding of the segment to the kinase domain, thus keeping the SU in an open conformation. Consequently, this kinase can later phosphorylate a neighboring SU in the same dodecamer (trans-phosphorylation). Persistence of this kinase active state is thought to be fundamental for the LTP process,[9,10] while a quick return to an inactive state (through lack of T286 phosphorylation) would not allow such a process. Rebinding of Ca/CaM to T305/306, which could stimulate a return to the

Received: September 15, 2017
Revised: October 18, 2017
Published: October 18, 2017

DOI: 10.1021/acs.jpcb.7b09214
J. Phys. Chem. B 2017, 121, 10344−10352

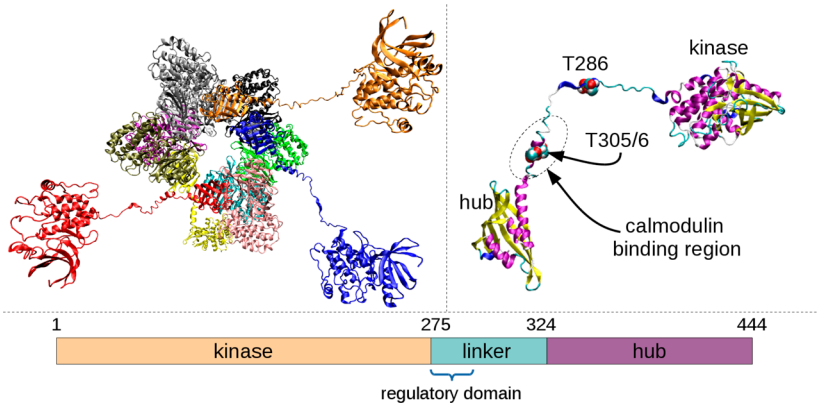

Figure 1. (Left panel) Modeled CaMKII dodecamer. It is a stack of two rings, each with six SUs, shown in different colors (one ring is behind the other; therefore, they are not clearly distinguishable). Eight of the SUs are in their closed conformations, while another four—blue, red, and orange in the front ring and yellow in the back (mostly hidden)—were modeled in the open state. (Right panel) Representation of one of the SUs, showing the hub and kinase subdomains, connected via a flexible linker, and highlighting T286, T305, and T306, phosphorylation sites known to be critical for the protein's function. (Lower panel) Schematic view of the three subdomains.

closed conformation, is prevented by the phosphorylation of either.[11−13] These two sites are also known to be related to LTP.[14]

The mechanism governing the process just described is not well understood at the molecular level. Using elastic network models and molecular dynamics (MD), we show in this study the effects of phosphorylation on the dynamics of the system and highlight the relevance of specific regions of the H, L, and K subdomains in determining the behavior of the protein.

We also inspect the stability of the system and evaluate the experimental observation of the spontaneous release of SUs upon activation. This release event is thought to be the way in which an activated SU can be dropped from an already active CaMKII molecule and later be inserted in an inhibited one, thus kick-starting its activation via transphosphorylation of the same enzyme's neighboring SUs.[15]

METHODS

The crystal structure with pdb code 3SOA[16] describes human CaMKII in its α isoform, with a β7 linker, in a closed or autoinhibited conformation. This isoform is the one with the highest concentration in neurons.[15] The 3SOA structure is the one that we used to form the closed SUs of the CaMKII dodecamer employed for our simulations. On the other hand, the 2WEL[17] pdb crystal structure contains a calmodulin-bound CaMKII in its δ isoform, in an open conformation. Because the kinase domains of both isoforms have a high sequence similarity—about 93%—we combined the hub of 3SOA with the linker and kinase domains of 2WEL to form open SUs. The numbering that we use for both open and closed SUs follows that of 3SOA, with the kinase being formed by residues 1−275 and the hub by 324−444. Finally, combining eight closed and four open SUs, a CaMKII dodecameric system, without calmodulin, was created, forming the initial model for our systems, as shown in Figure 1. The resulting simulation box contains, after solvation with TIP3P water,[18] more than 1.2 million atoms.

In order to drive the modeled molecule to a stable conformation, we ran several cycles of minimization and equilibration. The simulations in this work were performed using the AMBER15[19] software package, with all of them—except for the minimizations—using the GPU version of the PMEMD program. We employed the Amber12 force field. The systems were kept at a temperature of 298 K using Langevin dynamics with a collision frequency of 2 ps^{-1} and a pressure of 1 atm via a weak-coupling Berendsen barostat, with a relaxation time of 2 ps. The SHAKE algorithm was adopted, allowing the use of a 2 fs time step. The protocol followed for minimization and equilibration was (1) 100 cycles of minimization, using AMBER's XMIN method, followed by 5000 cycles using steepest descent and another 5000 steps using conjugate gradient and (2) 1 ns of heating to 298 K followed by 1 ns at constant T and P (1 atm) and finally 20 ns with constant T. This equilibrated structure was then used as a starting point for the construction of the three different systems that we studied, differing in the phosphorylation state of residues T286, T305. and T306: (1) a nonphosphorylated (NP) system, with no phosphorylation of those residues, (2) a phosphorylated (P) system, with phosphorylation of T286 in the four open SUs, and (3) an all-phosphorylated (AP) system, with the three mentioned residues phosphorylated, also in the four open SUs.

The addition of the phosphate group was achieved by replacing the involved threonines' side chains by phosphorylated ones: parametrized phosphothreonines with a single protonated phosphate group, THR-PO2(OH), with electric charge −1,[20,21] consistent with the AMBER family of force fields.

Once the P and AP systems were created by adding a phosphate group to T286 and T286,305,306, respectively, we repeated the equilibration protocol described before for each of the three new systems (including NP). We finally took the three last frames obtained for each system as the initial structures for the NP, P, and AP models.

From them, we started ∼400 ns long conventional MD (cMD) simulations, which constitute the three MD trajectories analyzed in this work. In addition, taking the initial 20 ns of these simulations, we calculated the average potential and dihedral energies of each of them and used that information to calculate the parameters needed to start an accelerated MD (aMD) simulation[22] for each system.

In summary, we ended up with three systems of CaMKII (NP, P, and AP), all of them with four open SUs and the other eight closed, and none of them contained calmodulin. For each system, we ran two simulations, one cMD and one aMD, obtaining, in the end, a total of six trajectories with an overall simulation time of about 2.4 μs (if we consider the acceleration

DOI: 10.1021/acs.jpcb.7b09214
J. Phys. Chem. B 2017, 121, 10344−10352

of the aMD trajectories, the effective simulation time becomes much longer).

RESULTS AND DISCUSSION

First 1% of ANM Modes Explains the Closed to Open Transition of Subunits. Elastic networks are idealized models of molecules that have been successful at explaining many dynamical aspects of proteins. In this work, we applied the Anisotropic Network Model (ANM)[23] to show how the system's normal modes (eigenvectors of the inverse Hessian matrix) overlap with the closed to open transition of CaMKII.

To this end, we formed the *transition vectors* by subtracting the coordinates of the closed from the open structure and vice versa: $\boldsymbol{T}_{\text{closed}}$ = open−closed and $\boldsymbol{T}_{\text{open}}$ = closed−open.

On the other hand, we performed an ANM calculation of the open and closed frames, obtaining the $3N$ modes (where N is the number of nodes in the elastic network, one per α-carbon) for each

$$\boldsymbol{V}_i^j = \text{mode } j \text{ of frame } i \qquad (i = \text{open, closed})$$

and corresponding frequencies. Next, we calculated the cumulative overlap of the ANM modes of frame i onto the transition vector of the same frame

$$\text{CUM}_i(j_{\max}) = \sum_{j=0}^{j_{\max}} \boldsymbol{V}_i^j \cdot \boldsymbol{T}_i$$

obtaining, thus, two CUM_i functions of $j_{\max}$, representing the overlap of the ANM modes onto the closed to open and open to closed transitions. Despite the complexity of the system—a dodecamer with large electrostatic interactions, as shown later—the cumulative functions, displayed in Figure 2, show

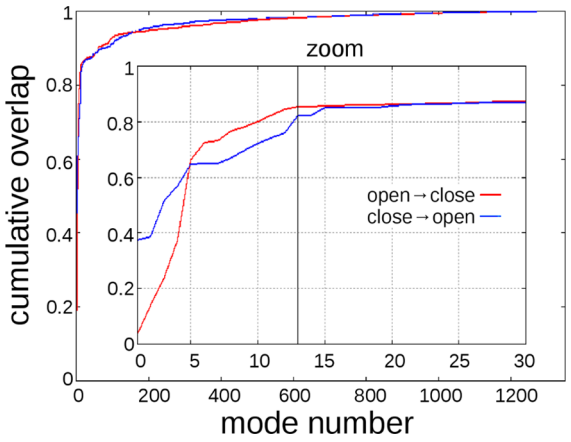

Figure 2. Cumulative overlap of ANM modes onto open to closed (red) and closed to open (blue) structures of SU1. The first 1% of the modes, 13 out of the total 1305, explains more than 80% of the overlap. The inset is a zoomed-in image of the first 30 modes.

that the first 1% of the total ANM modes (13 out of a total of 1305) is enough to explain 80% of the opening and closing of the SU. That is, the combination of the first 13 ANM modes is enough to span 80% of the space that the system covers when going from the closed to the open conformation. This is a result comparable to those obtained in previous studies, where it was found that a few percent of the ANM modes is responsible for the low-frequency motions of the system,[24,25] i.e., those motions that determine the main structural changes of the molecule. Turning the argument around, this fact also validates the construction and modeling of the open SUs.

Phosphorylation of Subunits Changes the Influence/Sensitivity Patterns of the Molecule. Figure 3 shows the normalized perturbation response scanning (PRS)[26,27] maps of the NP, P, and AP cases for the cMD plus aMD simulations. The element (i,j) in the PRS matrix expresses the response of residue j to a perturbation on residue i. Thus, column j of the matrix can be interpreted as the sensitivity profile of residue j (how strongly it responds to perturbations on other residues), and row i can be seen as the influence profile of residue i (how strongly it influences other residues).

In the figure, we can observe that the background response of the system does not change much, but there are specific regions that do change significantly. In the P case, there is a strong enhancement of the sensitivity of the kinases in open SUs (open kinases for short). This is seen in residues 1−275, about the first half in each SU, in SU6 and SU9, especially the latter. AP also presents enhancements in the open kinases corresponding to SU3, SU6, and SU9, although to a lesser extent. The fact that only open kinases increase their sensitivity is not surprising as core regions like hubs tend to be more influential, presumably due to their tight packing, while regions in the periphery—the open kinases—with less structural restraints tend to easily respond to perturbations in the core. This result is, hence, suggesting that phosphorylation tends to keep the SUs open, thus making them more sensitive.

Interestingly, the increase in kinase response, which can be associated with an increase in kinase activity, is significantly larger in the P case. A possible explanation of this somewhat counterintuitive effect will be developed in a later section. However, we note here that it is in agreement with the experimental results of Majeed et al.,[13] where they also observe enhanced kinase activity in the double phosphorylation scenario, AP, but it is the single one, P, that shows the largest increase. (We should mention that we are associating kinase activity with kinase sensitivity. The intuitive reason for this, which needs to be tested further, is that in order for a kinase to be active it needs to sense and react to the presence of its target, that is, it needs to be sensitive.)

As per the mechanisms involved in the increase of sensitivity, we turn now to the observation of the trajectories generated during the MD simulations. In the three cases, NP, P, and AP, the initially open structures do not go back to the closed conformation, but rather, they lean to the side, keeping the linker relatively stretched (see Figure 4). In most cases, the linker (and a few of the first amino acids of the kinase) of the open SU makes contact with a neighboring, closed, kinase. However, for SU6 in the P case (orange in the figure), due to the neighboring SU1 kinase (blue) also being open, the SU6 kinase leans on it, making full contact. This kinase−kinase interaction, with SU6 being on the outside and influenced by the other kinase, may be responsible for the enhanced sensitivity of the SU6 kinase *(a sensitive molecule on top of another sensitive one will become even more sensitive)*.

The high sensitivity of SU9, in the P case (yellow in the figure), on the other hand, has a different explanation. This kinase stayed, during all of the simulation time, away from other SUs. Because it is free from its neighbors, it has less spatial constraints and is thus expected to show high sensitivity in PRS. However, this may change if the simulation is continued longer because the chance of becoming in contact with neighbors will increase.

DOI: 10.1021/acs.jpcb.7b09214
J. Phys. Chem. B 2017, 121, 10344−10352

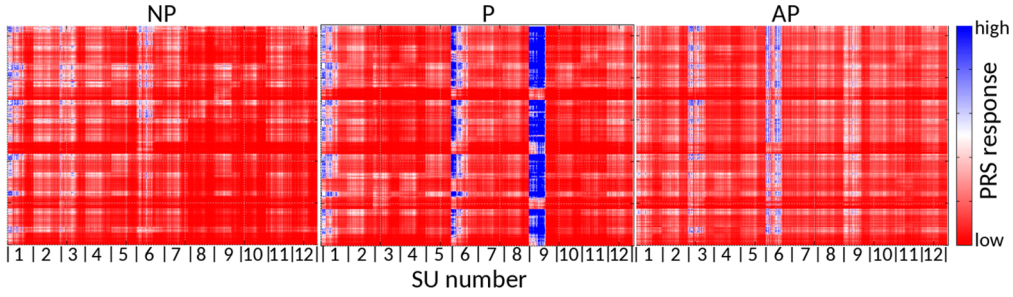

Figure 3. PRS matrices of the NP, P, and AP cases for the aMD simulations. The kinase subdomains of SU6 and SU9 show a highly increased response to perturbation in the system when T286 is phosphorylated. This is diminished if T286, T305, and T306 are simultaneously phosphorylated.

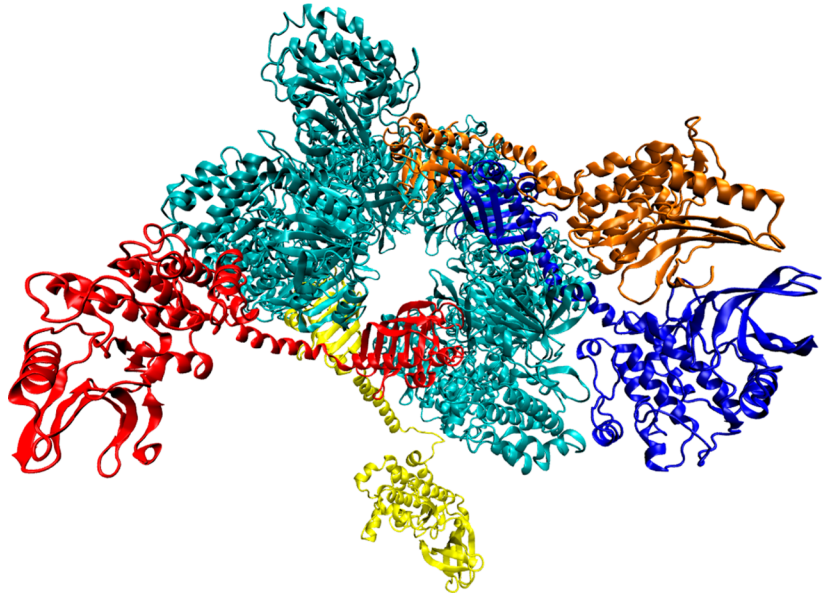

Figure 4. Last frame of the accelerated MD simulation of the CaMKII dodecamer, with the closed SUs in cyan and the open in different colors (SU1 blue, SU3 red, SU6 orange, SU9 yellow). The open SUs all tend to lean to the side and have their linkers and first part of kinase lying on the neighboring kinase. However, SU6 makes almost full contact with the SU1's linker and kinase, while SU9 remains away from its neighbors.

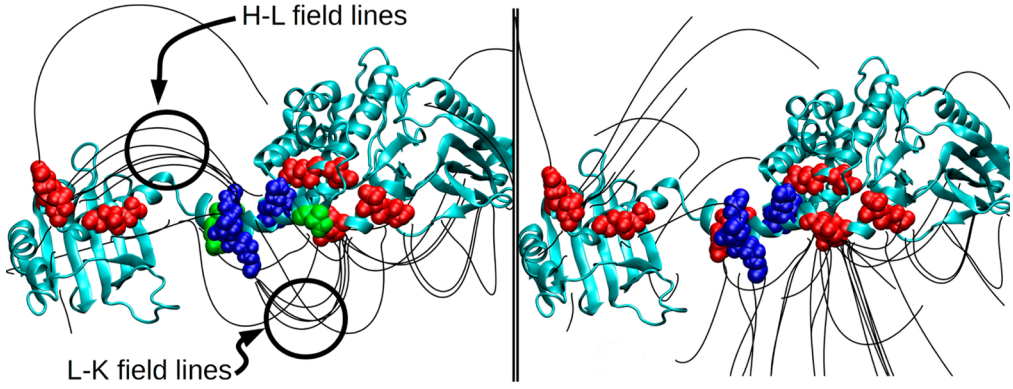

Figure 5. SU1 in the open conformation. Both the hub (H), on the left, and the kinase (K), on the right, contain negatively charged patches, shown in red, while the linker (L) presents a positively charged patch, shown in blue. The NP molecule is displayed in the left panel, showing a high density of electric field lines (shown in a circle), connecting the patches in H with L and those in L with K. T286, T305, and T306 are shown in green when in their NP form. The right panel shows the same structure but in the P case, where the organized structure of electric field lines connecting H with L and L with K is now lost, representing a lower electrostatic attraction between subdomains.

Three Electrically Charged Regions in the Hub, Linker, and Kinase Domains Determine the Electrostatic Equilibrium of the Subunits, Which Is Largely Disrupted by Phosphorylation. We performed an electrostatic analysis of individual SUs, solving the Poisson–Boltzmann equation[28] for six different structures, taken from the end of the trajectories of each simulation (NP, P, and AP; both cMD and aMD). The results show three important highly charged

DOI: 10.1021/acs.jpcb.7b09214
J. Phys. Chem. B 2017, 121, 10344–10352

Table 1. Conservation of Residues That Form Each of the Three Charged Patches[a]

hub	**E325**	**E329**	**D335**	**E337**	**K341**	**D344**	**E360**	**D363**
	E 88%	E 76%	D 96%	E 80%	K 86%	D 98%	E 91%	D 82%
	D 02%	D 08%		D 17%	R 13%			E 15%
linker	**K291**	**K292**	**R296**	**R297**	**K298**	**K300**		
	K 81%	K 95%	R 99%	R 99%	K 100%	K 98%		
	R 19%	R 05%				R 02%		
kinase	**E99**	**D100**	**E105**	**E109**	**D111**			
	E 96%	D 97%	E 97%	E 99%	D 96%			
	D 03%	E 02%			E 03%			

[a]The sequence location and identity of residues are in bold; the percentage indicates the frequency of occurrence of the given residue identity.

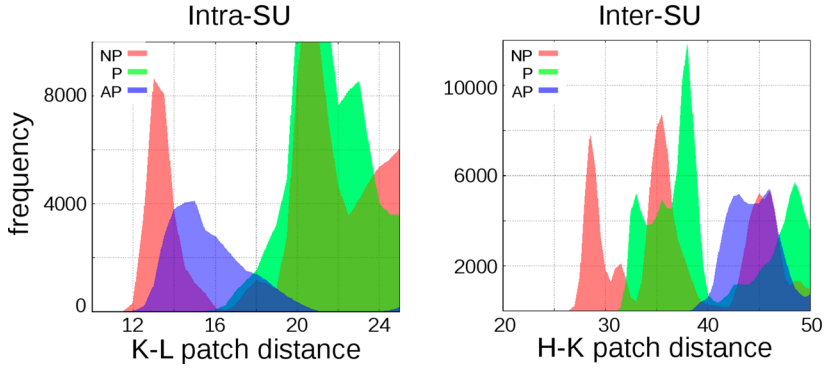

Figure 6. Normalized frequency distributions of the CoM distances of charged patches K and L of the same SU (left panel) and H and K of neighboring SUs (right panel). The NP case (red) has larger contributions for short separations, followed by P (green) and AP (blue), indicating the strong effect of phosphorylation in these distributions.

patches, one in each domain of the SUs, namely, E99, D100, E105, E109, and D111, in the kinase domain; K291, K292, R296, R297, K298, and K300 in the linker; and E325, E329, D335, E337, K341, D344, E360, and D363 in the hub domain. Figure 5 shows an *electrostatic pathway* of electric field lines of one of the open SUs, connecting the three patches represented in red and blue (corresponding to negative and positive charge, respectively). The pattern of field lines is highly organized in the NP case (left panel): a high density of lines (like the ones shown in circles) means that the end regions of those lines are strongly attracted to each other. Thus, the left panel shows strong electrostatic attraction between H and L and between L and K. However, that high-density pattern is largely disrupted in the AP case (right panel), and hence, the attraction between the domains is strongly weakened. This is intuitively explained by the presence of the three residues in the linker, T286, T305, and T306, being neutral in the NP case, while each of them acquires a negative charge in the AP case via phosphorylation. This results in a partial neutralization of the charged patch in L.

The aforementioned residues, E325, E329, E360, and D363, were also mentioned by Bhattacharyya et al.[29] as possibly involved in the linker's binding to the hub (their numbering scheme corresponds to the mouse sequence, as represented in the 1HKX pdb, and is slightly different from ours). As pointed out by them, these four residues line the groove formed between two neighboring hubs, where the linker finds a place to bind, facilitated by the electrostatic interaction between the negative patch in the hub and the positive residues in the NP linker. In this way, phosphorylation of T286 breaks the electrostatic attraction, thus reducing the linker's binding affinity to the groove.

In order to validate these results, we repeated the analysis using representative conformations for each simulation: for each of the six systems, the entire simulation data was divided in five root-mean-square deviation-based clusters using the average linkage algorithm in the cpptraj[30] analysis program. In each case, the cluster with the greatest population was selected as representative and APBS was applied to it, qualitatively reproducing the above results.

We must note that, although this is a true mechanism of action observed in the simulation, the dodecamer structure complicates matters, making it possible to mix patches of one SU with patches in a neighboring one. For example, in Figure 4, the H patch of SU1 (blue) interacts with the L patch of SU6 (orange). Still, the electrostatic mechanism and its alteration via phosphorylation remain valid.

Charged Patches in H, K, and L Are Highly Conserved. The strong electrostatic characteristics of the above-mentioned charged patches, one in each of the subdomains, H, K, and L, appear to imply their important role in the structure and/or dynamics of the system. This idea is further supported by the fact that all of the residues forming those patches have identities that are well conserved in a multiple sequence alignment (MSA), composed of 111 sequences, performed using the ConSurf Web site.[31] In fact, if the conservation calculation considers residues with the same charge as having the same identity (a rather reasonable assumption if the charge is what gives these patches their function, as we propose), then the conservation of every residue in the K and L domains is higher than 98%. In the H subdomain, it is larger than 96%, with the exception of E325, E329, and E360, which have conservation of 90, 84, and 91%, respectively, as displayed in Table 1. The first two residues show co-evolution between them: in the MSA, every time that E325 mutates, E329 also mutates (though the converse is not true). In summary, all of the amino acids in the three patches show either very strong conservation or co-

DOI: 10.1021/acs.jpcb.7b09214
J. Phys. Chem. B 2017, 121, 10344−10352

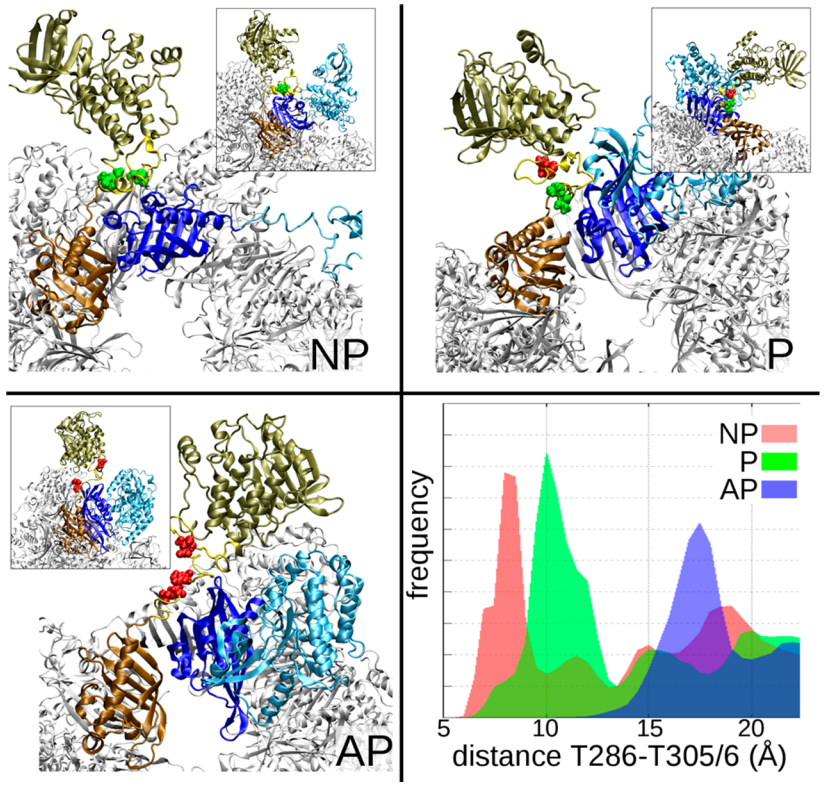

Figure 7. Detailed view of the positional relation between an open SU and a neighboring one, in the NP, P, and AP cases. Two SUs are shown, in brown and blue shades, along with the three phosphorylation sites, T286, 305, and 306, in red or green spheres, depending on whether they are phosphorylated. Each panel contains an inset with a rotated view of the same image. The AP case is distinguished from the other in that the T286 vs T305/306 distance is greatly increased (as a consequence of electrostatic repulsion). Also shown is a panel with a histogram of distances between those sites.

evolution, suggesting an important structural and/or functional role.

Intrasubunit K−L and Intersubunit H−K Charged Patches Tend to Stick Together in the NP Case: Autoinhibited Structures Do Not Need to be Fully Closed. From a structural point of view, the charged patches show their importance when the separation between them is analyzed. Considering all of the studied cases, a tendency toward very short separation between K and L patches belonging to the same SU is seen in the NP case. There is only one SU in the cMD and another one in the aMD simulation that stay apart around 45−50 Å (center of mass, CoM, distance). In all other cases, the shortest interatomic separations between patches are on the order of 10 Å, although they can get as close as 2 Å. Figure 6, left shows the distribution of CoM distances between the K and L patches for the three cases NP, P, and AP. For short distances—the regions in which we are interested—the first peak corresponds to the NP case, expressing its tendency to shorter K−L separations. These short distances are explained by the strong electrostatic attraction between the K and L patches. Upon phosphorylation, the negative charge acquired by L serves as a partial neutralization of the previously positively charged linker, which, in turn, disrupts the strong electrostatic pathway shown in Figure 5, resulting in less sticky K−L patches. Hence, the K−L distances tend to increase when phosphorylation is present. We should notice the somewhat counterintuitive result that the AP case is intermediate between those two, although one would expect it to be more pronounced (larger K−L separations). However, as previously mentioned in reference to the PRS maps, this result appears to be in agreement with that of Majeed et al.,[13] where they observed significantly enhanced kinase activity in the P case but lower enhancement in the AP case.

This difference in separation between subdomains is not observed in relation to the L and H patches, presumably due to the rigid nature of the hub—which constitutes the core of the CaMKII system—as opposed to the very flexible linker. The kinase, being on the periphery of the system, is less constrained and is able to follow the linker in its high-entropy trajectory, thus their charged patches staying in close proximity.

On the other hand, because a SU can become very long when in the open conformation, up to about 130 Å, it is not uncommon to find one stretching over another neighboring SU (as shown in Figure 4). In such cases, interactions between charged patches of neighboring SUs are important; moreover, this seems to be the norm rather than the exception as it is observed in virtually all of the SUs; their initially open linker−kinase tends to stretch to a side, more than to return to their closed conformation (this was not observed only in one SU of the P case, where the kinase lingered above of its corresponding hub). In particular, if we consider the separation between H and K patches of neighboring SUs (Figure 6, right panel), we observe that they are found closest in the NP case. Again, the explanation is the stronger H−L−K attraction when the system is not partially neutralized by phosphorylation. It is not really important if the interaction is intra- or intersubunit as the behavior appears to be determined only by the net charge of the involved patches, not by their belonging.

DOI: 10.1021/acs.jpcb.7b09214
J. Phys. Chem. B 2017, 121, 10344−10352

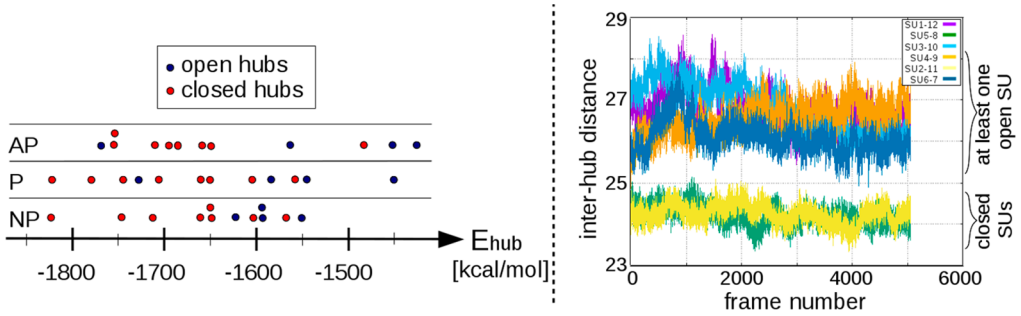

Figure 8. (Left panel) Self-energy of the hubs of each of the 12 SUs of the NP, P, and AP cases. The closed conformations (red points) tend to have less energy than the open ones (blue points), suggesting a higher stability. Average open/closed hub energy = −1573/−1668 kcal/mol → Δ(closed→open) = −95 ± 5 kcal/mol. (Right panel) Interhub distance for vertical dimers of hubs (first neighbors in different rings). The two cases where the two hubs correspond to closed SUs show a significantly lower separation (picture shows the NP-cMD case but is representative of all cases).

The minimum H−K CoM distances are about 26 Å for NP, 31 Å for P, and 38 Å for AP. These are relatively small differences, especially when considering the length of the open SU; visually, the P and NP conformations look alike. This suggests an alternative to the usual interpretation of the inactive state, where the inhibited SU is thought as being fully closed (H and K of the same SU bound to each other). In view of the right panel of Figure 6, we propose that an inactive state could also be related to a conformation where the SU is open but its kinase domain is attached to a neighboring hub, with separations between them of ∼26 Å. Also, the active state could be associated with the kinase separated by only a few more angstroms from that value (∼31 Å for P, 38 Å for AP). The former states resemble the *activation-competent conformations* observed by Myers et al.[32] using single-particle electron microscopy, that is, conformers where K domains are not attached to their corresponding H while not being in the active state.

Phosphorylation of T305/T306 May or May Not Enhance the Effect of Phosphorylating T286. As previously noted in relation to the PRS maps and the K−H distances, the change in behavior observed when going from the NP to the P case is compatible with the fact that the attraction of H−L−K is diminished upon phosphorylation. Thus, K can get a few more angstroms away from H, becoming more detached and, hence, more sensitive and with more freedom in its function as a kinase to *search* for a residue suitable for phosphorylation.

When also phosphorylating residues T305 and T306, we would, in principle, expect the above mechanism to be enhanced, but that is not what we have found (in agreement with Majeed et al.[13]), as previously analyzed and shown in Figures 3 and 6. Does MD provide an explanation for this unintuitive fact? We believe that it does.

Figure 7 shows a detailed view of the positional relation between an open SU and a neighboring one, in the different phosphorylation scenarios. There, the distance between the brown kinase and blue hub does not seem to greatly vary (compatible with Figure 6). Then, how can we explain the unexpected behavior of AP? Comparison of each image with its corresponding inset allows one to appreciate the separation between phosphorylation sites T286 and T305−306. We observe that their separation is greatly increased in the AP case (see also the first peak of each case in the last panel). The reason for this is simply, and once again, the electrostatic repulsion between the sites—fully phosphorylated in AP—while there was no repulsion at all in the NP and P cases (because NP has the three sites neutral and P has only T286 charged). If this distance was fixed, we would have a reason to expect the AP case to show an enhancement of the effects in P, but because the distance doubles in the AP case, we do not have a reason to expect such enhancement. What we actually see is the opposite, a sort of dampening of the effect, where the AP sensitivity (Figure 3) and the K−L distance (Figure 6, left) are intermediate between NP and P.

Hubs in Closed SUs Are More Stable Than Open Ones. Figure 8, left shows the total energy of each of the 12 hub subdomains of the dodecamer. Closed hubs tend to be lower in energy when compared to open ones, average ΔE(closed−open) = −95 ± 5 kcal/mol. In addition, within open SUs, it is observed that the P cases have a higher average energy, −1590, −1578 and −1551 kcal/mol for the NP, P, and AP cases, respectively. There are studies showing that activation of CaMKII negatively affects the stability of the core, leading to an eventual release of a SU.[15,29] Our results hint at this fact, that open conformations, particularly phosphorylated ones, tend to destabilize the core, favoring the release of the SU from the dodecamer.

This point should be studied further as we are ignoring entropic effects (which one should, in principle, include because what determines the stability of the system is its free energy, not its energy). These entropic effects will presumably reduce the separation between the open and closed SUs mentioned in the previous paragraph: the entropy of the hub in the closed case is arguably going to be lower than that of the open case because the subdomain is trapped between the neighboring hubs and the closed kinase, having less freedom to move; this would decrease its entropy and increase its free energy. Nevertheless, the large energetic difference of about 95 kcal/mol between the average open and closed hubs seems too large to be overcome by entropic effects, and thus, the closed form should remain more stable.

We have also observed that the interhub (first neighbors, in different rings) separation is significantly increased when one or two hubs belong to open SUs. This is represented in the right panel of Figure 8, where there is a very clear separation between cases with the two hubs corresponding to closed SUs (green and yellow lines, at the bottom) and other cases. The average change in separation is 2.3 ± 0.5 Å. This is in correspondence with the previous energetic result because a closer, tighter packing of the hubs is associated with a lower energy and, hence, increased stability. It should be noted that there is no

DOI: 10.1021/acs.jpcb.7b09214
J. Phys. Chem. B 2017, 121, 10344−10352

significant difference in separations among the NP, P, and AP cases.

CONCLUSIONS

In summary, with the goal of studying the closed and open conformations of the SUs and the effect of phosphorylation, we prepared six systems of CaMKII in dodecameric form, with eight closed and four open SUs. Two systems were wild-type nonphosphorylated, two had a phosphorylated T286, and two had phosphorylation in T286, T305, and T306. We chose those specific residues because they were mentioned in the literature as responsible for the trigger of signals related to activation of CaMKII. One of the systems of each of the mentioned states was used to perform conventional MD, while the other was the starting point of accelerated MD, which is capable of accelerating the dynamics, increasing the effective coverage of the conformational space by the simulation. In this way, we covered the possibility of not doing enough cMD to see important effects.

The main finding of the present study is the determination of three specific regions of the hub, linker, and kinase of every SU, characterized by a significant electric charge. These charged patches are shown to play an important role in the interactions between the subdomains, via a K−L−H electrostatic pathway formed by them, as shown in Figure 5. In particular, the NP case shows a strong interaction between H and L and between L and K. This is partially lost when T286 or T286, T305, and T306 acquire a phosphate group as their negative charge tends to neutralize the originally positive charge of the L patch, effectively weakening the interaction pathway.

The relevance of these charged regions is further supported by a conservation analysis of the identity of the amino acids forming the three patches. Table 1 shows the high conservation of each of those residues. However, when the analysis is done taking into account not the specific amino acid identity but rather their net electric charge, the conservation scores become much higher, in most cases above 97%. Also, the two residues that have the lowest conservation show a strong co-evolution between them. The existence of these patterns highlights the evolutionary importance of those regions being charged and strongly suggests that they are fundamental for the function of the molecule.

From a structural point of view, it is frequently speculated that the separation between K and H of the same SUs greatly increases upon activation and goes back to its original conformation when deactivated (not phosphorylated). This is not what we have observed: once the SUs are open, they do not go back to the initial closed conformations with K fully attached to H (although we do not discard this possibility as it may just be out of our simulation time scale). Rather, K and H stay apart, and their CoM separation is a bit larger for the P cases. The distance between the first peaks of the NP and AP cases in the left panel of Figure 6 is 2 Å. This means that the conformational changes occurring as a cause of phosphorylation are more subtle than usually thought. If we look at the separation between patches of neighboring SUs, the situation is similar in that the distance H−K is significantly lower for the NP case, followed by P and last the AP case (right panel of Figure 6). Again, this behavior can be rationalized by the stronger electric charge of the L patch in the NP case that acts as a *glue* between H and K. As phosphorylation neutralizes the charge of L, the glue weakens and the repulsion between the like charges in H and K starts to dominate, leading to an increased separation. This image is consistent with the *activation-competent conformations* observed by Myers et al.[32]

The overall picture arising from this study is that the three mentioned charged patches are key in enabling and disabling the interactions between the SUs' subdomains, both in an inter- and intra-SU fashion. When in the NP state, the interactions are fully operational, and there is a strong attraction that tends to keep the different domains close to each other. Upon phosphorylation, the charge of the L patch is partially neutralized, leading to a breakage of that attractive force; therefore, the kinase domain becomes looser. This leads to a few angstroms increase of the intra-SU K−L and inter-SU H−K separations. In turn, the hub, now being partially unbound from one side (the kinase side), experiences an increase in its self-energy, becoming less stable; this is particularly true for hubs in phosphorylated SUs because their energy is larger than the one of those on NP SUs (Figure 8). This, maybe coupled to a similar event on a neighboring SU, may lead to destabilization of the whole SU, ending in release of a monomer of CaMKII or perhaps a dimer, as noted in other studies.[15,29]

AUTHOR INFORMATION

Corresponding Author

*E-mail: ijgeneral@gmail.com.

ORCID

Ignacio J. General: 0000-0002-8346-6978

Author Contributions

¶F.P. and E.K.A. contributed equally to this work.

Notes

The authors declare no competing financial interest.

ACKNOWLEDGMENTS

We thank Prof. Ivet Bahar for helpful discussions and for her support. We also acknowledge Agencia Nacional de Promocion Cientifica y Tecnologica for their grants PICT-2015-1706 (E.K.A.) and PICT-2015-3832 (I.J.G.).

REFERENCES

(1) Anderson, M. Calmodulin kinase signaling in heart: an intriguing candidate target for therapy of myocardial dysfunction and arrhythmias. *Pharmacol. Ther.* **2005**, *106*, 39−55.

(2) Fährmann, M.; Kaufhold, M. A. Functional partitioning of epithelial protein kinase CaMKII in signal transduction. *Biochim. Biophys. Acta, Mol. Cell Res.* **2006**, *1763*, 101−109.

(3) Skelding, K. A.; Rostas, J. A.; Verrills, N. M. Controlling the cell cycle: the role of calcium/calmodulin-stimulateed protein kinases I and II. *Cell Cycle* **2011**, *10*, 631−639.

(4) Lin, M. Y.; Zal, T.; Ch'en, I. L.; Gascoigne, N. R. J.; Hedrick, S. M. A pivotal role for the multifunctional calcium/calmodulin-dependent protein kinase II in T cells: From activation to unresponsiveness. *J. Immunol.* **2005**, *174*, 5583−5592.

(5) Lisman, J. Holoenzymes: Refreshing memories. *eLife* **2014**, *3*, No. e02041, DOI: 10.7554/eLife.02041.

(6) Tombes, R. M.; Faison, M. O.; Turbeville, J. M. Organization and evolution of multifunctional Ca(2+)/CaMdependent protein kinase genes. *Gene* **2003**, *322*, 17−31.

(7) Bayer, K. U.; De Konick, P.; Schulman, H. Alternative splicing modulates the frequency-dependent response of CaMKII to Ca^{2+} oscillations. *EMBO J.* **2002**, *21*, 3590−3597.

(8) Wang, P.; Wu, Y.-L.; Zhou, T.-H.; Sun, Y.; Pei, G. Identification of alternative splicing variants of the β subunit of human Ca^{2+}/calmodulin-dependent protein kinase II with different activities. *FEBS Lett.* **2000**, *475*, 110.

DOI: 10.1021/acs.jpcb.7b09214
J. Phys. Chem. B 2017, 121, 10344−10352

(9) De Koninck, P.; Schulman, H. Sensitivity of CaM kinase II to the frequency Ca2+ oscillations. *Science* **1998**, *279*, 227−230.
(10) Giese, K. P.; Fedorov, N. B.; Filipkowski, R. K.; Silva, A. J. Autophosphorylation at Thr286 of the alpha calcium-calmodulin kinase II in LTP and learning. *Science* **1998**, *279*, 870−873.
(11) Hanson, P. I.; Schulman, H. Inhibitory autophosphorylation of multifunctional Ca2+/calmodulin-dependent protein kinase analyzed by site-directed mutagenesis. *J. Biol. Chem.* **1992**, *267*, 17216−17224.
(12) Colbran, R. J. Inactivation of Ca2+/calmodulin-dependent protein kinase II by basal autophosphorylation. *J. Biol. Chem.* **1993**, *268*, 7163−7170.
(13) Majeed, A. B. B.; Pearsall, E.; Carpenter, H.; Brzozowski, J. S.; Dickson, P. W.; Rostas, J. A. P.; Skelding, K. A. CaMKII kinase activity, targeting and control of cellular functions: Effect of single and double phosphorylation of CaMKIIα. *Calcium Signaling* **2014**, *1*, 36−51.
(14) Elgersma, Y.; Fedorov, N. B.; Ikonen, S.; Choi, E. S.; Elgersma, M.; Carvalho, O. M.; Silva, A. J.; et al. Inhibitory autophosphorylation of CaMKII controls PSD association, plasticity, and learning. *Neuron* **2002**, *36*, 493−505.
(15) Stratton, M.; Lee, I.-H.; Bhattacharyya, M.; Christensen, S. M.; Chao, L. H.; Schulman, H.; Groves, J. T.; Kuriyan, J. Activation-triggered subunit exchange between camkii holoenzymes facilitates the spread of kinase activity. *eLife* **2014**, *3*, No. e01610, DOI: 10.7554/eLife.01610.
(16) Chao, L. H.; Stratton, M. M.; Lee, I.-H.; Rosenberg, O. S.; Levitz, J.; Mandell, D. J.; Kortemme, T.; Groves, J. T.; Schulman, H.; Kuriyan, J. A Mechanism for tunable autoinhibition in the structure of a human Ca 2+ /calmodulin-dependent Kinase II holoenzyme. *Cell* **2011**, *146*, 732−745.
(17) Rellos, P.; Pike, A. C. W.; Niesen, F. H.; Salah, E.; Lee, W. H.; von Delft, F.; Knapp, S. Structure of the CaMKIIdelta/Calmodulin complex reveals the molecular mechanism of CaMKII kinase activation. *PLoS Biol.* **2010**, *8*, e1000426.
(18) Jorgensen, W. L.; Chandrasekhar, J.; Madura, J. D.; Impey, R. W.; Klein, M. L. Comparison of simple potential functions for simulating liquid water. *J. Chem. Phys.* **1983**, *79*, 926−935.
(19) Case, D. A.; Berryman, J. T.; Betz, R. M.; Cerutti, D. S.; Cheatham, T. E., III; Darden, T. A.; Duke, R. E.; Giese, T. J.; Gohlke, H.; Goetz, A. W.; et al.. *AMBER 2015*; University of California: San Francisco, CA, 2015.
(20) Homeyer, N.; Horn, A. H. C.; Lanig, H.; Sticht, H. AMBER force field parameters for phosphorylated amino acids in different protonation states: Phosphoserine, phosphothreonine, phosphotyrosine and phosphohistidine. *J. Mol. Model.* **2006**, *12*, 281−289.
(21) Bryce, R. A. *AMBER Parameter Database*. http://sites.pharmacy.manchester.ac.uk/bryce/amber (2017).
(22) Hamelberg, D.; Mongan, J.; McCammon, J. A. Accelerated molecular dynamics: A promising and efficient simulation method for biomolecules. *J. Chem. Phys.* **2004**, *120*, 11919−11929.
(23) Atilgan, A. R.; Durell, S. R.; Jernigan, R. L.; Demirel, M. C.; Keskin, O.; Bahar, I. Anisotropy of fluctuation dynamics of proteins with an elastic network model. *Biophys. J.* **2001**, *80*, 505−515.
(24) Bahar, I.; Lezon, T. R.; Bakan, A.; Shrivastava, I. H. Normal mode analysis of biomolecular structures: Functional mechanisms of membrane proteins. *Chem. Rev.* **2010**, *110*, 1463−1497.
(25) Das, A.; Gur, M.; Cheng, M. H.; Jo, S.; Bahar, I.; Roux, B. Exploring the conformational transitions of biomolecular systems using a simple two-state anisotropic network model. *PLoS Comput. Biol.* **2014**, *10*, e1003521.
(26) Atilgan, C.; Atilgan, A. R. Perturbation-response scanning reveals ligand entry-exit mechanisms of ferric binding protein. *PLoS Comput. Biol.* **2009**, *5*, e1000544.
(27) General, I. J.; Liu, Y.; Blackburn, M.; Mao, W.; Gierasch, L.; Bahar, I. ATPase subdomain IA is a mediator of interdomain allostery in Hsp70 molecular chaperones. *PLoS Comput. Biol.* **2014**, *10*, e1003624.
(28) Dolinsky, T. J.; Nielsen, J. E.; McCammon, J. A.; Baker, N. A. PDB2PQR: An automated pipeline for the setup, execution, and analysis of Poisson-Boltzmann electrostatics calculations. *Nucleic Acids Res.* **2004**, *32*, W665−W667.
(29) Bhattacharyya, M.; Stratton, M. M.; Going, C. C.; McSpadden, E. D.; Huang, Y.; Susa, A. C.; Elleman, A.; Cao, Y. M.; Pappireddi, N.; Burkhardt, P.; et al. Molecular mechanism of activation-triggered subunit exchange in Ca(2+)/calmodulin-dependent protein kinase II. *eLife* **2016**, *5*, No. e13405, DOI: 10.7554/eLife.13405.
(30) Roe, D. R.; Cheatham, T. E., III. PTRAJ and CPPTRAJ: Software for processing and analysis of molecular dynamics trajectory data. *J. Chem. Theory Comput.* **2013**, *9*, 3084−3095.
(31) Celniker, G.; Nimrod, G.; Ashkenazy, H.; Glaser, F.; Martz, E.; Mayrose, I.; Pupko, T.; Ben-Tal, N. ConSurf: Using evolutionary data to raise testable hypotheses about protein function. *Isr. J. Chem.* **2013**, *53*, 199−206.
(32) Myers, J. B.; Zaegel, V.; Coultrap, S. J.; Miller, A. P.; Bayer, K. U.; Reichow, S. L. The CaMKII holoenzyme structure in activation-competent conformations. *Nat. Commun.* **2017**, *8*, 15742.

DOI: 10.1021/acs.jpcb.7b09214
J. Phys. Chem. B 2017, 121, 10344−10352